When SOFC-based cogeneration systems become convenient? A cost-optimal analysis

Energy Reports 8 (2022) 8709–8721

Contents lists available at ScienceDirect

Energy Reports

journal homepage: www.elsevier.com/locate/egyr

Research paper

When SOFC-based cogeneration systems become convenient? A cost-optimal analysis

Paolo Marocco *, Marta Gandiglio, Massimo Santarelli

Department of Energy, Politecnico di Torino, Corso Duca degli Abruzzi 24, 10129 Torino, Italy

ARTICLE INFO

Article history:
Received 15 April 2022
Received in revised form 23 May 2022
Accepted 15 June 2022
Available online xxxx

Keywords:
SOFC
Fuel cell
Cogeneration
Energy efficiency
Modelling
Optimal design

ABSTRACT

SOFC-based cogeneration systems potentially offer high energy efficiency and reduced environmental burden, but further research is needed for successful product commercialization. This study has been performed within the framework of the EU project Comsos (Commercial-scale SOFC systems), whose aim is to validate and demonstrate fuel cell-based cogeneration systems for building applications. A Mixed Integer Linear Programming (MILP) model was developed to address the optimal design and scheduling of the SOFC-based energy system. Main techno-economic data of the SOFC modules were provided by the manufacturers and validated through the ComSos installations. The analysis was applied to non-residential applications, focusing on the supermarket sector, which is characterized by interesting features for SOFC systems, e.g., the presence of a constant electrical baseload over the whole year. The main goal of this work is to assess the influence of different parameters, including SOFC investment cost, stack lifetime and efficiency, to identify the conditions that make the SOFC technology cost-effective. The Spark Spread (SS) impact was also investigated to point out the most suitable geographical regions for the installation of SOFC cogeneration systems.

The SOFC profitability was found to be highly dependent on its investment cost and the value of the spark spread. An SOFC cost of around 1.2 k€/kW is needed to make this technology profitable for SS equal to -0.05 €/kWh; while a CAPEX of around 6 k€/kW is sufficient for the SOFC to be chosen in the cost-optimal configuration when SS is 0.1 €/kWh (with stack lifetime of 5 years). Compared to the case with no SOFC, the levelized cost of electricity is reduced by 46% if the spark spread is 0.1 €/kWh and the SOFC cost is 1.2 k€/kW, which is a reasonable CAPEX for scenarios with high SOFC production volumes.

1. Introduction

The rising costs of fossil fuels and the need for reduced harmful emissions are the main drivers to pursue more efficient and sustainable methods of power and heat generation. As reported by the International Energy Agency (IEA) (IEA, 2019), buildings account for around 30% of final energy use and over 55% of global electricity consumption. Moreover, energy consumption in buildings is increasing with an annual average growth rate of 1.1%. Buildings are also responsible for 28% of total energy-related CO_2 emissions. The building sector is thus crucial for achieving the European Union (EU)'s energy and environmental goals. The EU has established a legislative framework that includes the Energy Performance of Building Directive (EPBD) (European Union, 2021a) and the Energy Efficiency Directive (EED) (European Union, 2021b). In this context, cogeneration is considered as an efficient solution that enables better use of fuel energy to provide heating and electricity to buildings (Fubara et al., 2014). Among the different Combined Heat and Power (CHP) technologies, Fuel Cells (FCs) can offer improved energy efficiency and reduced environmental burden, thus attracting great attention in recent years (Ammermann et al., 2015).

FC-based CHP systems for residential buildings have been analysed in many literature works. Ellamla et al. (2015) carried out a review about the current status of FC cogeneration systems for the residential sector. The authors reported that Proton Exchange Membrane Fuel Cells (PEMFCs) and Solid Oxide Fuel Cells (SOFCs) are the most suitable FC technologies for cogeneration. However, they also highlighted that the main disadvantage of fuel cells is related to their high capital expense, which is primarily due to their low production volumes. Low system lifetime and high capital costs are, at present, the main bottlenecks in the development of FC micro-CHP systems (Arsalis, 2019). Sorace et al. (2017) investigated the feasibility of an FC cogeneration system coupled with a heat pump for a residential case study. They performed an energy and economic analysis considering different configurations based on PEMFC and SOFC technologies.

* Corresponding author.
E-mail address: paolo.marocco@polito.it (P. Marocco).

https://doi.org/10.1016/j.egyr.2022.06.015

The results of their analysis revealed that the SOFC option was able to achieve the lowest operating costs, because of the higher efficiency of SOFCs compared to PEMFCs. However, investment in the SOFC configuration was found to be less convenient because of the higher capital cost of this technology. Napoli et al. (2015) also presented a comparison between PEMFC and SOFC CHP systems for the residential sector. They observed that both technologies were able to reduce primary energy consumption for the electrical and thermal needs of domestic users, with further improvements when installing an energy storage system. The SOFC system was preferable from an energy point of view because of its higher global efficiency; however, it was characterized by a greater upfront cost compared to the PEMFC alternative. Caramanico et al. (2021) showed that the high SOFC investment cost made this solution not convenient for residential systems, even though SOFCs led to economic savings in the operational phase due to their promising performance. Adam et al. (2015) reviewed various options for heat recovery from PEMFCs and SOFCs, concluding that FC micro-CHP solutions can provide significant energy and cost savings in residential dwellings.

The installation of FCs has also been analysed in non-residential buildings, which possess interesting features, e.g., the presence of a constant baseload through all the year (Accurso et al., 2021). Whiston et al. (2021) carried out an expert elicitation study about the market for stationary solid oxide fuel cells and reported that commercial-scale systems are the most favourable entry-level market in the United States (US). McLarty et al. (2016) analysed the integration of stationary FCs into the US commercial building stock. They found that buildings with large baseloads, such as supermarkets and hotels, benefit most from the installation of fuel cells. Accurso et al. (2021) analysed the techno-economic feasibility of SOFC-based CHP solutions for the hotel and hospital sector and showed that, despite the high capital expenditures, the SOFC option can become cost-effective with the help of subsidies. Studies about SOFC installations in different types of public buildings in China have been addressed in the literature (Tan et al., 2018; Jing et al., 2017).

SOFC-based cogeneration systems can also lead to environmental benefits. Alns and Sleiti (2021) investigated SOFC CHP solutions for commercial buildings, reporting cost savings and reductions in CO_2 emissions by 30%, NO_x by 90% and SO_2 by 90%. Hormaza-Mejia et al. (2017) reported reduced Greenhouse Gas (GHG) emissions when considering an SOFC micro-CHP system with integrated thermal storage for residential applications. Similarly, Fong and Lee (2016) found that SOFC-based micro-cogeneration resulted in a 30.8% reduction in CO_2 emissions compared to the conventional system. CO_2 emissions reductions of up to 62% were computed for SOFC CHP systems installed in mid-size office buildings (Naimaster and Sleiti, 2013).

This work has been carried out in the framework of the ComSos (Commercial-scale SOFC systems) project (ComSos, 2018), whose aim is to validate and demonstrate FC-based systems in the mid-size range. An optimization framework, based on the Mixed Integer Linear Programming (MILP) technique, was developed to perform the optimal design and scheduling of SOFC-based multi-energy systems. The main goal is to identify the techno-economic conditions that make the installation of SOFC systems economically convenient. Thus, the influence of various parameters has been assessed, including electricity price, gas price and SOFC-related data, such as investment cost, efficiency, and stack lifetime. Main technical and economic data of the SOFC technology were provided by the SOFC manufacturers involved in ComSos. Real part-load performance curves of the SOFC stack were also implemented in the optimization routine for a more accurate simulation of the SOFC performance. To the best of our knowledge, such a comprehensive investigation, also strengthened by high-quality input data from real SOFC systems, has not been found in the previous literature.

The structure of this study is the following: Section 2 describes the methodology that has been adopted for the optimal design of the energy system. The objective function of the optimization framework is then derived in Section 3, while in Section 4 the reference case study is introduced. In Section 5, the main results are shown and discussed, performing a sensitivity analysis on different techno-economic parameters. Finally, conclusions are reported in Section 6.

2. Energy system modelling

Fig. 1 shows the scheme of the energy system to be designed. The fuel cell component operates in cogeneration mode, producing both electrical and thermal energy to satisfy the building demands. The electrical demand of the building can be covered by electricity purchased from the electrical grid, fuel cell operation, or battery discharging. Instead, the thermal demand can be covered through a gas boiler powered by Natural Gas (NG) from the gas grid, fuel cell operation or thermal storage discharging. A sensible hot water tank was considered as thermal storage.

An MILP-based approach was employed to address the optimal design of the poly-generative energy system. More specifically, the model is able to compute the optimal sizing of the energy system along with its optimal hourly scheduling over the entire time horizon (T). A 1 year time horizon with hourly resolution was considered in this study.

The optimization problem was formulated in MATLAB environment using IBM CPLEX as solver. Simulations were carried out on a desktop computer with an Intel(R) Core(TM) i7-4770 CPU at 3.4 GHz and 32 GB RAM.

Input parameters to the optimization framework are the following:

- The electrical demand $\forall t \in T$
- The thermal demand $\forall t \in T$
- The cost of electricity from the grid $\forall t \in T$
- The cost of natural gas from the grid $\forall t \in T$
- Techno-economic data of the various components that are involved in the energy system, i.e., Fuel Cell (FC), Battery Storage (BS), Gas Boiler (GB) and Thermal Storage (TS).

The following decision variables are computed:

- The sizes of all the components of the energy system, i.e., FC, BS, GB and TS
- The input power of the FC and GB, i.e., the gas power that is bought from the gas grid, $\forall t \in T$
- The output power of the FC (electrical and thermal) and GB (thermal) $\forall t \in T$
- The on and off status of the FC and GB $\forall t \in T$
- The charging and discharging power of the BS and TS $\forall t \in T$
- The amount of energy that is stored in the BS and TS $\forall t \in T$
- The electrical power that is bought/sold from/to the electrical grid $\forall t \in T$.

At any time interval, the electrical power balance is given by the following relationship:

$$P_{FC,out,el}(t)+P_{BS,dc}(t)+P_{GR,buy,el}(t) = P_{BS,ch}(t)+P_{GR,sell,el}(t)+P_{LD,el}(t) \quad (1)$$

where $P_{FC,out,el}$ (in kW) is the electrical power at the FC outlet, $P_{BS,dc}$ (in kW) is the battery discharging power, $P_{GR,buy,el}$ (in kW) is the imported electrical power, $P_{BS,ch}$ (in kW) is the battery

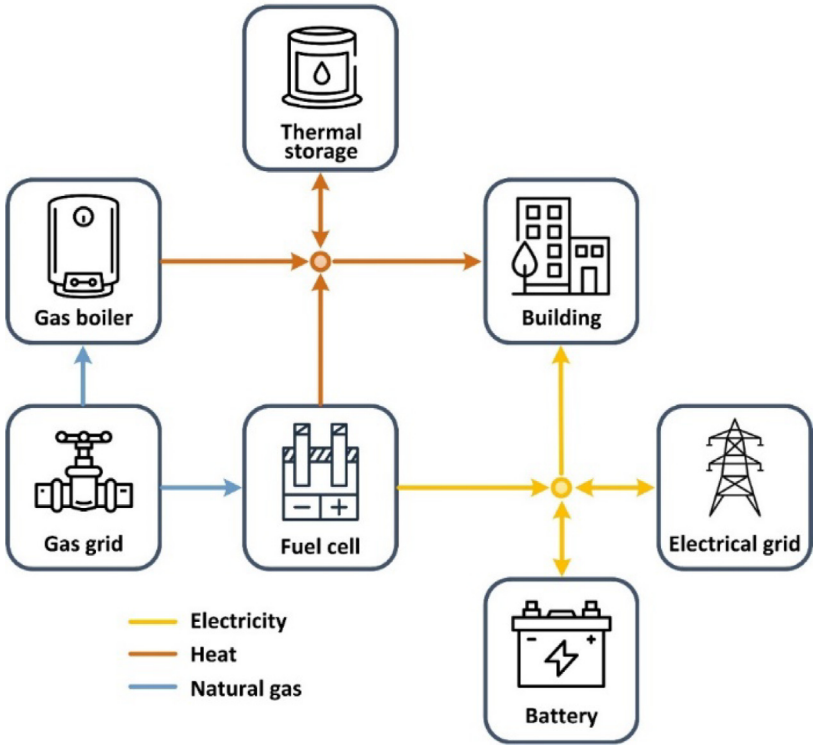

Fig. 1. General layout of the SOFC-based cogeneration system.

charging power, $P_{GR,sell,el}$ (in kW) is the exported electrical power (in kW), and $P_{LD,el}$ (in kW) is the electrical load to be covered.

The thermal power balance was instead defined as follows:

$$P_{FC,out,th}(t)+P_{GB,out}(t)+P_{TS,dc}(t) = P_{TS,ch}(t)+P_{LS,th}(t)+P_{LD,th}(t) \quad (2)$$

where $P_{FC,out,th}$ (in kW) is the thermal power at the FC outlet, $P_{GB,out}$ (in kW) is the thermal power at the gas boiler outlet, $P_{TS,dc}$ (in kW) is the TS discharging power, $P_{TS,ch}$ (in kW) is the TS charging power, $P_{LS,th}$ (in kW) is the dissipated thermal load (power loss), and $P_{LD,th}$ (in kW) is the thermal load to be covered. The $P_{LS,th}$ term was added to always satisfy the thermal power balance. It was assumed that the $P_{LS,th}$ term is dissipated; however, it could represent a possible revenue if there is, for example, a district heating network to which the excess heat can be sold.

The size of the FC and GB component (i.e., rated power in kW) was treated as a continuous variable that is allowed to vary within a certain size range, as reported below (with i = FC, GB):

$$P_{i,rated,min} \leq P_{i,rated} \leq P_{i,rated,max} \quad (3)$$

Similarly, the size of the energy storage devices (i.e., storage capacity in kWh) was constrained as follows (with i = BS, TS):

$$Cap_{i,min} \leq Cap_i \leq Cap_{i,max} \quad (4)$$

The lower size limit of each component was set to zero, which means that a certain technology is selected in the system configuration whenever the MILP simulation returns a value of its size greater than zero.

2.1. Fuel cell

Eq. (5) sets the constraints on the minimum and maximum operating power of the fuel cell (in terms of electrical power):

$$y_{FC,min} \cdot P_{FC,rated,aux}(t) \leq P_{FC,out,el}(t) \leq y_{FC,max} \cdot P_{FC,rated,aux}(t) \quad (5)$$

where the terms $y_{FC,min}$ and $y_{FC,max}$ are the lower and upper bounds of the FC modulation range. $P_{FC,rated,aux}$ is an auxiliary variable that is defined as:

$$P_{FC,rated,aux}(t) = P_{FC,rated} \cdot \delta_{FC}(t) \quad (6)$$

where $P_{FC,rated}$ (in kW) is the FC rated power and δ_{FC} is a binary variable that is equal to 1 if the FC is on or 0 if off. The introduction of the $P_{FC,rated,aux}$ variable is required to transform the product of $P_{FC,rated}$ and δ_{FC} in the following set of linear inequalities:

$$P_{FC,rated,aux}(t) \leq P_{FC,rated} - (1 - \delta_{FC}(t)) \cdot P_{FC,rated,min} \quad (7)$$

$$P_{FC,rated,aux}(t) \geq P_{FC,rated} - (1 - \delta_{FC}(t)) \cdot P_{FC,rated,max} \quad (8)$$

$$P_{FC,rated,aux}(t) \leq P_{FC,rated,max} \cdot \delta_{FC}(t) \quad (9)$$

$$P_{FC,rated,aux}(t) \geq P_{FC,rated,min} \cdot \delta_{FC}(t) \quad (10)$$

Starting from the FC electrical efficiency curve (i.e., electrical efficiency as a function of the outlet electrical power), a performance curve that relates the outlet electrical power to the inlet gas power was derived. This performance curve was then modelled by means of a Piecewise Affine (PWA) approximation. According to the PWA approach, the FC performance curve (which relates the outlet electrical power to the inlet power) was approximated by means of p line segments. The positions of the related $p + 1$ breakpoints were found by performing an optimization problem (Gabrielli et al., 2016). The PWA approximation was then implemented within the MILP framework according to the process detailed in Marocco et al. (2021b). The following constraint was applied for each i-th line segment of the performance curve, $i \in \{1, \ldots, p\}$:

$$P_{FC,out,el}(t) \leq \alpha_{FC,el,i} \cdot P_{FC,in}(t) + \beta_{FC,el,i} \cdot \delta_{FC}(t) \quad (11)$$

where $P_{FC,in}$ (in kW) is the FC inlet power (in terms of gas), $\alpha_{FC,el,i}$ is the slope of the i-th segment and $\beta_{FC,el,i}$ (in kW) is the intercept of the i-th segment. Eq. (11) was then rearranged as:

$$P_{FC,out,el}(t) \leq \alpha_{FC,el,i} \cdot P_{FC,in}(t) + c_{\beta,FC,el,i} \cdot P_{FC,rated,aux}(t) \quad (12)$$

The expression for the estimation of $\alpha_{FC,el,i}$ and $c_{\beta,FC,el,i}$ can be found in Appendix A.

The thermal power generated by the fuel cell was instead expressed as follows:

$$P_{FC,out,th}(t) = \eta_{FC,th} \cdot P_{FC,in}(t) \tag{13}$$

where $\eta_{FC,th}$ is the fuel cell thermal efficiency, which was evaluated by means of linear approximation.

2.2. Gas boiler

The modulation range of the gas boiler was imposed through Eq. (14):

$$y_{GB,min} \cdot P_{GB,rated,aux}(t) \leq P_{GB,out}(t) \leq y_{GB,max} \cdot P_{GB,rated,aux}(t) \tag{14}$$

where $y_{GB,min}$ and $y_{GB,max}$ define the modulation range of the gas boiler. The $P_{GB,rated,aux}$ variable is described by the following equation:

$$P_{GB,rated,aux}(t) = P_{GB,rated} \cdot \delta_{GB}(t) \tag{15}$$

where $P_{GB,rated}$ (in kW) is the GB rated power and δ_{GB} is a binary variable that is equal to 1 if GB is operating and 0 otherwise. Eqs. (7) to (10), adapted for the GB, were then used for a linear representation of the product between $P_{GB,rated}$ and δ_{GB}.

The thermal power generated by the gas boiler was assessed through Eq. (16), where $P_{GB,in}$ is the GB inlet power (i.e., the imported gas power) and η_{GB} is the GB efficiency, which was assumed to be constant in this analysis.

$$P_{GB,out}(t) = \eta_{GB} \cdot P_{GB,in}(t) \tag{16}$$

2.3. Battery storage

The behaviour of the battery storage was modelled through the following linear dynamics:

$$E_{BS}(t) = E_{BS}(t-1) \cdot (1-\sigma_{BS}) + \eta_{BS,ch} \cdot P_{BS,ch}(t-1) \cdot \Delta t - \frac{P_{BS,dc}(t-1) \cdot \Delta t}{\eta_{BS,dc}} \tag{17}$$

where E_{BS} (in kWh) is the stored energy, σ_{BS} is the battery self-discharge coefficient, $\eta_{BS,ch}$ is the battery charging efficiency, $\eta_{BS,dc}$ is the battery discharging efficiency and Δt is the duration of the time interval.

The operation of the battery storage was also bounded between a minimum and maximum State-Of-Charge (SOC) value as described by Eq. (18). The SOC parameter is defined as the ratio of the stored energy to the rated capacity of the storage system. A minimum SOC value higher than 0 was set to mitigate the degradation of the battery over time.

$$Cap_{BS} \cdot SOC_{BS,min} \leq E_{BS}(t) \leq Cap_{BS} \cdot SOC_{BS,max} \tag{18}$$

A periodicity constraint was also added to impose the same storage level at the beginning and at the end of the time horizon.

2.4. Thermal storage

The approach described by Steen et al. (2015) was considered for the modelling of the thermal storage system. At each time step, the energy that is stored in the hot water sensible TS was expressed as:

$$E_{TS}(t) = E_{TS}(t-1) \cdot \left(1-\sigma_{TS,1}\right) - \sigma_{TS,2} \cdot \varphi_{TS} \cdot Cap_{TS} + \eta_{TS,ch} \cdot P_{TS,ch}(t-1) \cdot \Delta t - \frac{P_{TS,dc}(t-1) \cdot \Delta t}{\eta_{TS,dc}} \tag{19}$$

where E_{TS} (in kWh) is the stored energy, $\eta_{TS,ch}$ is the TS charging efficiency and $\eta_{TS,dc}$ is the TS discharging efficiency. The parameters $\sigma_{TS,1}$, $\sigma_{TS,2}$ and φ_{TS} have been introduced to model the TS losses, which depend on the amount of energy stored in the TS, the rated capacity of the TS and the ambient temperature. The φ_{TS} parameter was defined as a function of the minimum temperature (T_{min}), maximum temperature (T_{max}) and ambient temperature (T_{amb}), as follows (Steen et al., 2015):

$$\varphi_{TS} = \frac{T_{min} - T_{amb}}{T_{max} - T_{min}} \tag{20}$$

As reported by Eq. (21), the SOC of the thermal storage was imposed to vary within a certain range.

$$Cap_{TS} \cdot SOC_{TS,min} \leq E_{TS}(t) \leq Cap_{TS} SOC_{TS,max} \tag{21}$$

Finally, analogously to the battery, a periodicity constraint on the stored energy was also introduced for the thermal storage.

3. Objective function assessment

The objective function of the optimization problem is the total Net Present Cost (NPC) of the system (in €). As shown in Eq. (22), the NPC is the present value of all the costs incurred by the system over its lifetime, including capital (CAPEX) and operating (OPEX) expenditures, minus the present value of the salvage revenues.

$$C_{NPC} = C_{NPC,capex} + C_{NPC,opex} - C_{NPC,salv} \tag{22}$$

The $C_{NPC,capex}$ cost takes place at the beginning of the analysis period. It was computed as the sum of the capital expenditures of all the components that are involved in the energy system, i.e., BS, FC, GB and TS. The relationship for the estimation of the operating expenditures was expressed as follows (with i = BS, FC, GB, TS):

$$C_{NPC,opex} = \sum_{j=1}^{n} \frac{\sum_i C_{opex,i,j} + C_{GR,buy,el,j} - C_{GR,sell,el,j} + C_{GR,buy,gas,j}}{(1+d)^j} \tag{23}$$

where the subscript j represents the j-th year of the simulation, $C_{opex,i,j}$ is the annual OPEX of the i-th component, $C_{GR,buy,el,j}$ is the annual cost due to the electricity purchased from the grid, $C_{GR,sell,el,j}$ is the annual revenue from the sale of electricity to the grid, $C_{GR,buy,gas,j}$ is the annual cost due to the gas purchased from the grid (to feed both FC and GB), d is the discount rate, and n (in years) is the lifetime of the project. The $C_{opex,i,j}$ term was defined as a fraction of the CAPEX of the i-th component (the value of the percentage fraction varies according to the component). $C_{opex,i,j}$ also includes replacement costs if the i-th component must be replaced during the j-th year. The following expression was used to evaluate the $C_{GR,buy,el,j}$ term (in €/yr):

$$C_{GR,buy,el,j} = \sum_{t=1}^{8760} \left(P_{GR,buy,el}(t) \cdot c_{GR,buy,el}(t)\right) \tag{24}$$

where $P_{GR,buy,el}$ (in kW) is the electricity purchased from the electrical grid and $c_{GR,buy,el}$ (in €/kWh) is the related electricity price. Similarly, the annual cost associated with the imported gas was assessed by means of the following equation (in €/yr):

$$C_{GR,buy,gas,j} = \sum_{t=1}^{8760} \left(P_{GR,buy,gas}(t) \cdot c_{GR,buy,gas}(t)\right) \tag{25}$$

where $c_{GR,buy,gas}$ (in €/kWh) is the gas price and $P_{GR,buy,gas}$ (in kW) is the gas purchased from the gas grid, which is the sum of the

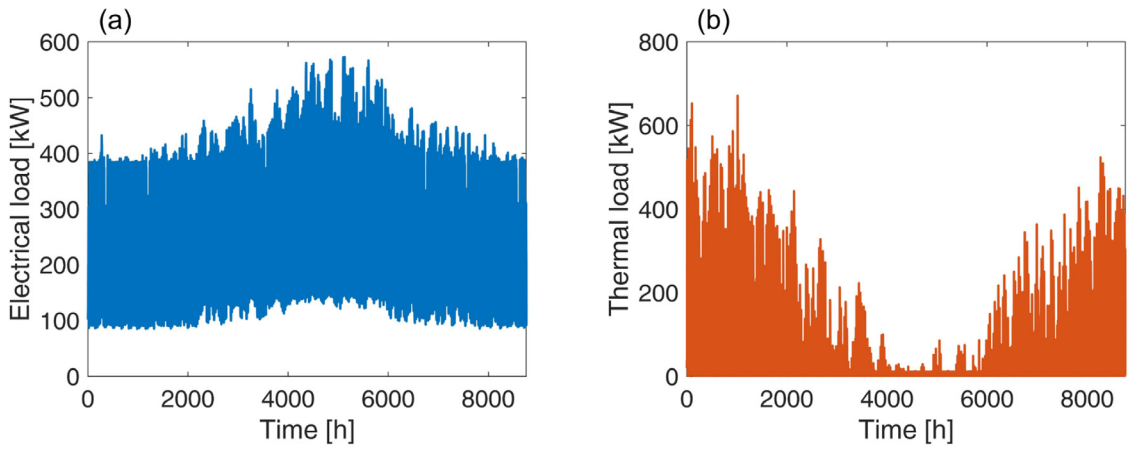

Fig. 2. Electrical (a) and thermal (b) load profiles of the reference case study over the year.

imported gas to power the FC and GB components, as reported by Eq. (26).

$$P_{GR,buy,gas}(t) = P_{FC,in}(t) + P_{GB,in}(t) \tag{26}$$

A constant price of the exported electricity (i.e, $c_{GR,sell,el}$ in €/kWh) was adopted for the estimation of the $C_{GR,sell,el,j}$ contribution.

The average price of electricity and gas was used to evaluate the Spark Spread (SS) parameter, whose expression is reported in Eq. (27) (Market Observatory for Energy, 2019). The 0.5 value that appears in Eq. (27) is the reference efficiency for conventional power plants.

$$SS = c_{GR,buy,el,avg} - \frac{c_{GR,buy,gas,avg}}{0.5} \tag{27}$$

The salvage value of a certain i-th component, i.e., $C_{salv,i}$ (in €), takes place at the end of the project lifetime (n). It was assumed this term to be proportional to the remaining lifetime of the component (Marocco et al., 2021a). The salvage value of a component was set to zero if its lifetime is equal to or greater than n. The present value of the overall salvage contribution, which appears in Eq. (22), was computed as follows:

$$C_{NPC,salv} = \frac{\sum_i C_{salv,i}}{(1+d)^n} \tag{28}$$

In the post-processing phase, focusing on the electrical-side control volume (see Fig. 1), the Levelized Cost Of Electricity (LCOE) was also assessed to further compare the various system scenarios. The LCOE has been evaluated as the ratio between the overall discounted costs for the electricity production and the discounted electrical energy supplied to the building. The overall costs include CAPEX and OPEX of the FC and BS systems, natural gas purchased for the SOFC operation, electricity bought from the grid, revenues (for the electricity sold to the grid and salvage values) and savings (for the heat recovered from the FC) (Beckers et al., 2013).

4. Reference case study

The presented MILP-based methodology has been applied to the case study of a supermarket, located in North Italy (Milan, IT) as base case. Commercial and retail buildings, such as supermarkets, are interesting end-users for the SOFC technology since they usually require a constant electrical demand over time, due to the refrigeration equipment. The availability of a baseload well matches with an SOFC system, whose optimal operating strategy is typically based on a continuous operation with reduced thermal cycles (Marocco et al., 2019).

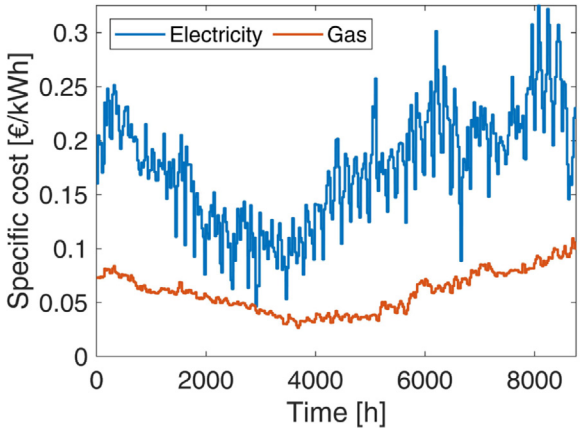

Fig. 3. Cost of electricity and gas over the year.

The supermarket hourly load profiles (electrical and thermal) have been retrieved from Wilson (2014), because robust electrical and thermal hourly load demand profiles are not available for the EU/IT area. The chosen dataset contains load profile data for 16 commercial building types and residential buildings in all TMY3 locations in the United States. The Typical Meteorological Year (TMY3) provides one year of hourly data that best represents median weather conditions over a multiyear period for a particular location.

The selected load profiles refer to a supermarket that has a floor area of 45,000 ft ^{2} (with one single floor) and is located in the city of St. Louis (Missouri, US). The location has been chosen since it has the same climatic zone as the city of Milan (IT) according to the Köppen–Geiger classification (Rubel et al., 2017) (humid subtropical climate *cfa*: warm temperate, no dry season, hot summer). Consequently, the case study is also representative of a typical supermarket located in Central-Southern Europe.

Electrical and thermal load profiles for the reference year are shown in Fig. 2. The electrical baseload is evident on the left graph (Fig. 2a), where around 85 kW are requested for the refrigeration (24/7 operating throughout the year). The peaks are due to the opening-dependent equipment such as lighting. A seasonal trend is also visible, with a higher demand during the summer period, due to the cooling load. The total electrical load (2402 MWh/yr) is mainly due to the supermarket facilities (around 70% of the load), followed by interior equipment, light, fans and cooling. As shown in Fig. 2b, the thermal load suffers from a strong seasonal variation, due to the heating season, while the minor continuous load is due to the domestic hot water. The total thermal demand

Table 1
Techno-economic assumptions of the battery storage component.

Parameter	Value	Ref.
Charging efficiency	0.95	Marocco et al. (2021a)
Discharging efficiency	0.95	Marocco et al. (2021a)
Self-discharge coefficient (stored energy)	5%/month	Gracia et al. (2018)
SOC range	0.2 to 1	Marocco et al. (2021a)
Lifetime of the BS module	10 yr	Crespi et al. (2021)
Lifetime of the BOP	Project lifetime	Assumption
Investment cost	450 €/kWh	Lamagna et al. (2021)
Replacement cost (% of Inv. cost)	50%	Schopfer et al. (2018)
OPEX fixed (% of Inv. cost)	2%/yr	Crespi et al. (2021)

Table 2
Techno-economic assumptions of the SOFC component.

Parameter	Value	Ref.
Electrical efficiency	Efficiency curve	Langnickel et al. (2020)
Thermal efficiency	Efficiency curve	Langnickel et al. (2020)
Lifetime of the stack (current value)	5 yr	Accurso et al. (2021), Whiston et al. (2021)
Lifetime of the BOP	Project lifetime	Assumption
Modulation range (% of rated power)	30 to 100%	McPhail et al. (2017), Gandiglio et al. (2018)
Investment cost (current value)	11,980[a] €/kW	Accurso et al. (2021)
Replacement cost (% of Inv. cost)	45%	ComSos (2018)
OPEX fixed (% of Inv. cost)	1%/yr	Caramanico et al. (2021)

[a]Including commissioning & installation costs.

Table 3
Techno-economic assumptions of the gas boiler component.

Parameter	Value	Ref.
Efficiency	95%	Gandiglio et al. (2014)
Lifetime	Project lifetime	Assumption
Modulation range (% of rated power)	15 to 95%	Ferroli Industrial Heating (2021)
Investment cost	125 €/kW	Ferroli Industrial Heating (2021)
OPEX fixed (% of Inv. cost)	3%/yr	Giarola et al. (2018)

Table 4
Techno-economic assumptions of the thermal storage component.

Parameter	Value	Ref.
Charging efficiency	0.95	Gabrielli (2019)
Discharging efficiency	0.95	Gabrielli (2019)
Self-discharge coefficient $\sigma_{TS,1}$	0.057%	Steen et al. (2015)
Self-discharge coefficient $\sigma_{TS,2}$	0.056%	Steen et al. (2015)
Minimum temperature	40 °C	ComSos (2018)
Maximum temperature	65 °C	ComSos (2018)
SOC range	0 to 1	Gabrielli et al. (2018)
Lifetime	Project lifetime	Assumption
Investment cost	104 €/kWh	Ferroli Industrial Heating (2021)
OPEX fixed (% of Inv. cost)	2%/yr	Assumption

Table 5
Other techno-economic assumptions.

Parameter	Value	Ref.
Discount rate	4%	Assumption
Commissioning & installation costs (% of Inv. cost)	10%	Napoli et al. (2015)
Project lifetime	20 yr	Assumption

(692 MWh/yr) is dominated by the gas used for the heating system (with a share higher than 90%), followed by the interior equipment and the domestic hot water.

The annual average costs of electricity and natural gas (in €/kWh) have been retrieved from the Eurostat database for non-household consumers (Eurostat - Data Explorer, 2022a,b) and include both the energy price and all the taxes and levies for Italy. An hourly profile has been then produced following the real costs trends for Italy during 2020 (Gestore Mercati Energetici (GME), 2022). The hourly cost trends of electricity and natural gas for the reference year are shown in Fig. 3. In this scenario, the resulting SS, evaluated according to Eq. (27), is equal to 0.055 €/kWh. In Section 5, a sensitivity analysis on SS will be performed to evaluate the influence of this parameter on the profitability of the SOFC investment.

The main techno-economic assumptions that have been used in this work are summarized in Tables 1 to 4, referring to the battery, fuel cell, gas boiler and thermal storage, respectively. The tables include, for each component, technical and economic information (e.g., efficiency, lifetime, modulation range, investment and operating costs) and related sources. Table 5 shows other general economic assumptions such as the plant lifetime, the discount rate and the commissioning and installation cost. The latter term has been applied to all the components except for the SOFC system, whose cost already includes the contribution due to commissioning and installation (Accurso et al., 2021).

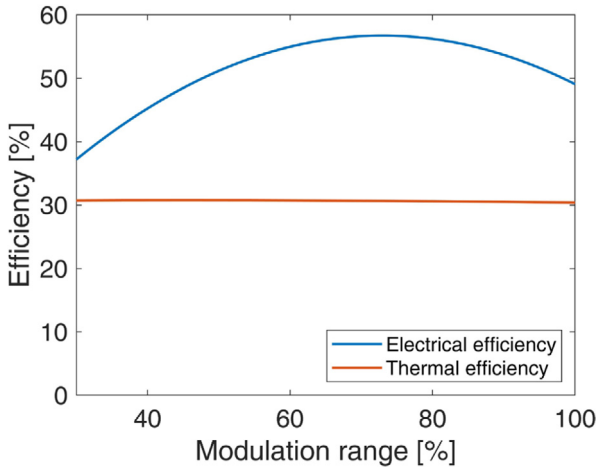

Fig. 4. Current electrical (blue) and thermal (red) efficiency curve of the SOFC component. (For interpretation of the references to colour in this figure legend, the reader is referred to the web version of this article.)

Table 2 shows data (investment cost, stack lifetime and efficiency) for the SOFC system in the current scenario: projections and target values will be deeply analysed in Section 5. The SOFC system is also characterized by variable performance depending on the operating point, following the electrical (blue line) and thermal (red line) efficiency curves shown in Fig. 4. Electrical and total efficiency trends were retrieved and fitted from the results of a real industrial FC installation, performed in the framework of the European DEMOSOFC project (Langnickel et al., 2020) (which is also in line with results from Comsos framework). In this context, a 100 kW SOFC system was operated for over 14,000 h (Gandiglio et al., 2020). The thermal efficiency (red line) shown in Fig. 4 has been evaluated as the difference between total and electrical efficiency (both available in Langnickel et al., 2020). The efficiency curves have been then converted into performance curves modelled by means of a PWA approximation, as explained in Section 2.1.

5. Results and discussion

The optimal design of the energy system was first performed considering the current techno-economic data of the SOFC technology. For the sake of comparison, a scenario with target values, derived in the framework of the Comsos project, was also carried out. The SOFC input parameters of the two scenarios are summarized in Table 6. A 70% reduction in the cost of the SOFC system is expected, as well as a two-fold increase in the stack lifetime. The value of the target electrical efficiency at rated power was computed assuming a 15% increase in the current rated value. The 15% increase was set according to the manufacturers' target values provided in the framework of the Comsos project data collection (Gandiglio et al., 2018). The difference between the target and current rated value (Δ) was then used to derive the curve of the target electrical efficiency. More specifically, all points in the current electrical efficiency curve (see Fig. 4) have been moved upwards by a value equal to Δ so as to preserve the curve shape (Gandiglio et al., 2018). Table 6 also shows the resulting value of the maximum electrical efficiency, which changes from 56.7% to 64.1%. The target thermal efficiency was assessed starting from the target electrical efficiency and hypothesizing unchanged the overall efficiency (i.e., the sum of electrical and thermal efficiencies).

The main sizing results of the two scenarios are reported in Table 7. It can be noted that, at present, it is not economically convenient to install SOFC systems. In the optimized system configuration, all the electrical demand is covered by imported electricity from the grid and all the thermal demand is covered by the gas boiler, fed by imported NG, with the support of a thermal storage. This results in a levelized cost of electricity of around 0.172 €/kWh. As shown in Fig. 5a, most of the NPC in the Current scenario is due to the electricity purchased from the grid, which accounts for roughly 86.5% of the total cost. The second main contribution is the purchase of natural gas from the grid to power the gas boiler (11.2% of the NPC), whereas the costs due to the thermal storage and gas boiler are almost negligible (2.3% of the NPC).

Table 6
Techno-economic parameters of the Current and Target scenarios.

Parameter	Current	Target Comsos
Investment cost SOFC system	11,980 €/kW	3340 €/kW
SOFC stack lifetime	5 yr	10 yr
Electrical efficiency at rated power	49.1%	56.4%
Maximum electrical efficiency	56.7%	64.1%

As reported in Table 7, the presence of an SOFC system becomes economically advantageous in the Target scenario, where it is suggested to install 255 kW of SOFC modules. This size value corresponds approximately to the average annual value of the building's electrical power demand. The SOFC-based system leads to an increase in the costs linked to the system components, which, unlike the Current scenario, are no longer negligible. In fact, the total SOFC cost, i.e., sum of SOFC CAPEX, OPEX and replacement contributions, accounts for 22.2% of the NPC. In the Target scenario, the purchase of natural gas is the highest cost share (almost half the NPC) since, compared to the Current scenario, the gas consumption increases to run the SOFC (from 763 to 3,322 MWh/yr). However, the SOFC operation makes it possible to reduce the amount of electricity purchased from the grid (from 2,042 to 649 MWh/yr), which is responsible for only 26.2% of the NPC. As shown in Table 7, it should also be noted that the FC-based CHP leads to a reduction in the GB rated power (from 514 to 416 kW) and TS capacity (from 371 to 334 kWh). Moreover, the battery is not present in either the Current or Target scenario, since its installation is not economically convenient considering its current investment cost and no grid operating constraints.

Fig. 5b shows that, at the beginning of the project lifetime, the Target scenario is more expensive than the Current one due to the high upfront cost of the SOFC technology. However, the SOFC operation allows the operating costs to be reduced, making the Target scenario cheaper starting from the sixth year (relative payback time).

After proving that the SOFC technology becomes convenient when SOFC target values are reached, a sensitivity analysis was carried out to better investigate the influence of the main SOFC- (CAPEX, stack lifetime and efficiency) and market-related (spark spread) parameters.

Fig. 6 reports the optimal FC size as a function of the investment cost of the FC system, for different values of FC stack lifetime and spark spread. FC CAPEX reduction up to 90% of the current value has been considered in this study. Indeed, costs of the FC system as low as 1 k€/kW have been reported with growing production volumes and further R&D (Ammermann et al., 2015; Battelle Memorial Institute, 2016). The SS parameter was varied from −0.05 to 0.1 €/kWh so as to cover the value of most European countries, as displayed in Appendix B (Fig. B.1). Spark spread values close to zero or negative correspond to countries where the electricity cost is comparable (or even lower) than the natural gas one. On the contrary, a high SS represents countries with an electricity cost higher than that of NG. The FC stack lifetime was also analysed in the range from 5 (current) to 10 (target) years.

It can be noted that the spark spread has a significant impact on the optimal sizing results. Considering an SS value of

Table 7
Main results of the Current and Target scenarios.

Scenarios	FC [kW]	GB [kW]	BS [kWh]	TS [kWh]	$E_{GR,buy,el}$ [MWh/yr]	$E_{GR,sell,el}$ [MWh/yr]	$E_{GR,buy,gas}$ [MWh/yr]	LCOE [€/kWh]	NPC [M€]
Current	0	514	0	371	2,041.7	0	763.4	0.172	6.48
Target Comsos	255	416	0	334	649.3	2.4	3,321.7	0.138	5.53

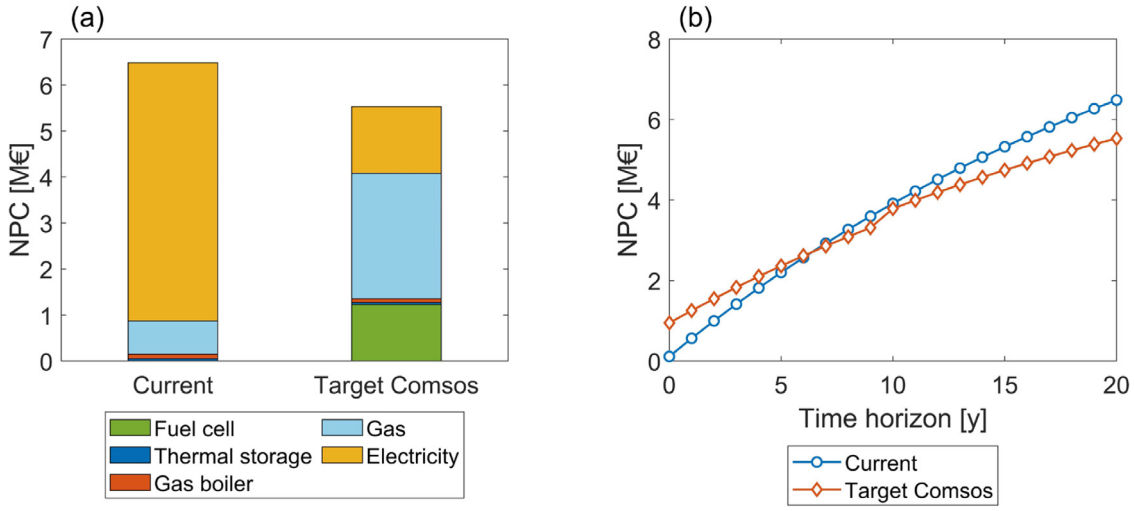

Fig. 5. (a) Breakdown of the NPC (at the end of the project lifetime) of the Current and Target scenarios. (b) NPC over the project lifetime of the Current and Target scenarios. The SS of the case study is 0.055 €/kWh (Italy). Electricity share (on the left graph) corresponds to the net value between the imported and the exported electricity (the revenue due to exported electricity is zero in the Current scenario and negligible in the Target one).

−0.05 €/kWh (Fig. 6a), it is profitable to install the FC-based CHP system only if the SOFC cost is around 1.2 to 2.4 k€/kW, i.e., a reduction of the current CAPEX by at least 80%. The cost of the fuel cell at which its installation becomes convenient increases as the SS increases. Concerning the 5 year lifetime case (blue bars of Fig. 6), a 90% cost reduction is required for the SOFC to become convenient with SS equal to −0.05 €/kWh, whereas a reduction of only half of the current CAPEX is sufficient for the FC to be chosen in the optimal system configuration if SS is 0.1 €/kWh. The benefits of a longer stack lifetime are also evident in Fig. 6, where it is shown that a higher value of this parameter facilitates the entry of the SOFC in the cost-optimal configuration. For example, in order for the SOFC to be profitable in scenarios with SS of 0.1 €/kWh (Fig. 6d), the current cost of the fuel cell should be reduced by 50% if the FC stack life is 5 years and by 30% if the FC stack life is 10 years. It is also noteworthy that the optimal FC size varies considerably with the variation of SS. In fact, when SS is −0.05 €/kWh, the maximum FC rated power is around 85 kW, which is close to the electrical baseload of the building (see Fig. 2a). The fuel cell size increases up to more than 400 kW when SS is 0.1 €/kWh. This size value corresponds approximately to the maximum electrical power demand of the building, except for the share related to the load increase in the summer period.

Fig. 7 shows the LCOE as a function of the FC CAPEX and for different SS values, with FC stack lifetime of 5 years. A decrease in the LCOE is connected to the installation of the SOFC system, whose effectiveness improves significantly as the spark spread increases. With SS equal to −0.05 €/kWh, which is close to that of Finland and Sweden (see Fig. B.1), the LCOE is reduced by only 0.4% when the FC cost drops from the current value (around 12 k€/kW) to 1.2 k€/kW. On the contrary, considering 0.1 €/kWh as SS, reducing the FC CAPEX by 90% leads to a decrease in the LCOE from 0.172 to 0.093 €/kWh, i.e., 46% LCOE reduction. Therefore, SOFC-based cogeneration systems are particularly suitable for countries with a high spark spread, such as Denmark, the United Kingdom and Germany, where SS is close to 0.1 €/kWh or even higher (see Fig. B.1).

The breakdown of the NPC by varying the FC CAPEX is displayed in Fig. 8 for different SS scenarios. The SOFC is not installed at its current cost, and the resulting NPC is around 6 to 7 M€, which is mainly due to the electricity purchased from the grid and, secondly, the gas to power the gas boiler. The largest cost share is thus represented by the operating expenses, whereas the total cost of the thermal storage and gas boiler is almost negligible. The SOFC system allows the cost of imported electricity to be reduced, which is more evident as the FC CAPEX decreases and the spark spread increases. As shown in Fig. 8d, this electricity cost becomes almost negligible when the FC CAPEX is around 1.2 k€/kW and SS is 0.1 €/kWh. The FC presence also leads to an increase in the NPC due to FC-related costs (i.e., FC CAPEX, OPEX and periodic stack replacements) and operating costs for imported natural gas. However, these higher expenses are justified by the lower cost related to the imported electricity, which results in a net decrease in the total NPC. It can be observed that, with SS equal to 0.05 and 0.1 €/kWh, the cost share due to the FC decreases when the FC CAPEX falls below 3.6 k€/kW, even if the size of installed FC increases (see Fig. 6). This is because the positive effect of a lower specific FC CAPEX (k€/kW) prevails over the increase in costs linked to the greater FC size.

It was also found that, in scenarios highly favourable for the SOFC, i.e., low FC CAPEX and high SS, the fuel cell system is used to convert natural gas into electricity that is both consumed by the building and sold to the grid, as shown in Fig. 8d (negative contribution, i.e., revenues, due to exported electricity).

Finally, the effect of the SOFC efficiency and stack lifetime on the LCOE is displayed in Fig. 9, considering SS equal to 0.05 €/kWh (which is close to the average European SS). It can be noted that, compared to the case with enhanced efficiency (red curve), the benefit of longer lifetime (orange curve) is more relevant at higher FC CAPEX values. By decreasing the investment cost of the SOFC (i.e., lower impact of replacement costs), the LCOE difference between the improved efficiency case and improved lifetime case decreases, until reaching an LCOE of around 0.125 €/kWh for both cases (which corresponds to a 27% reduction in LCOE compared to the current scenario).

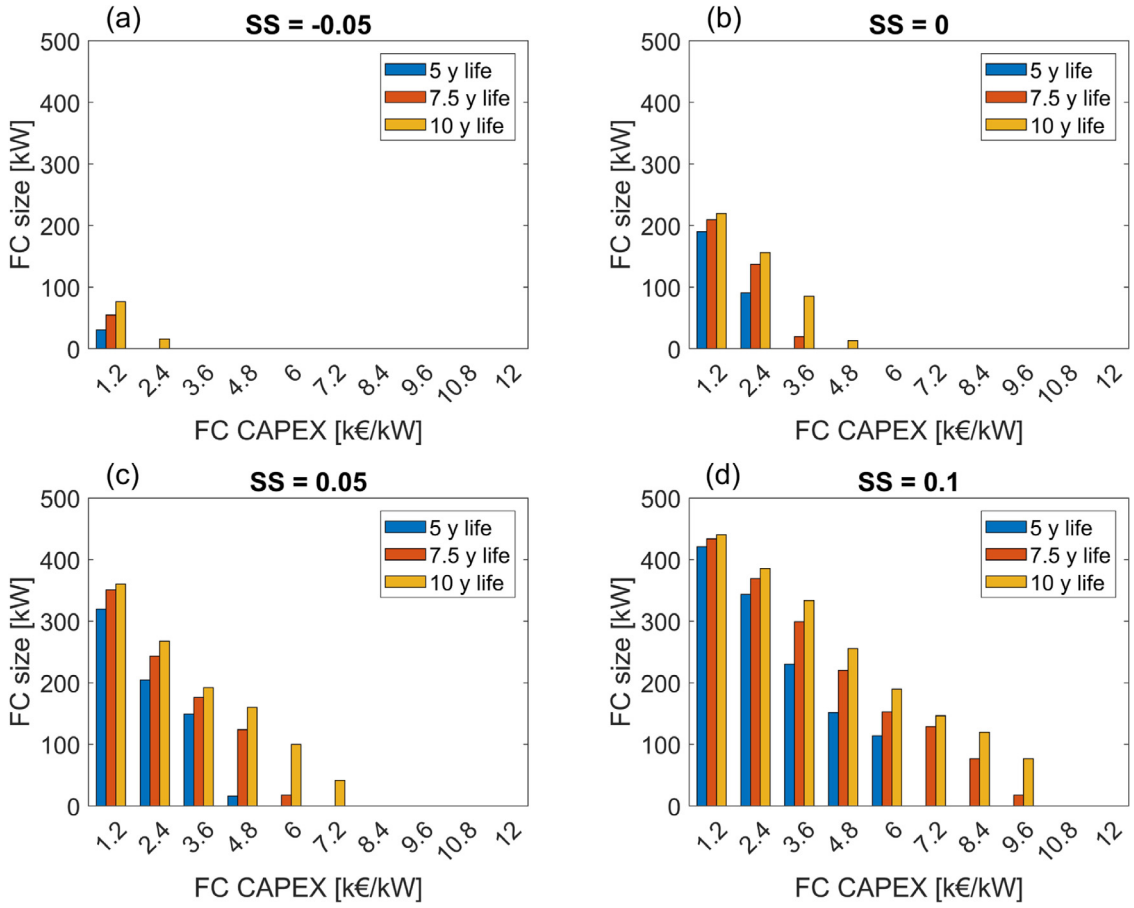

Fig. 6. FC size as a function of the FC CAPEX for different FC stack lifetime values and spark spread values: SS = −0.05 (a), SS = 0 (b), SS = 0.05 (c), and SS = 0.1 €/kWh (d). The current FC efficiency curve is considered. (For interpretation of the references to colour in this figure legend, the reader is referred to the web version of this article.)

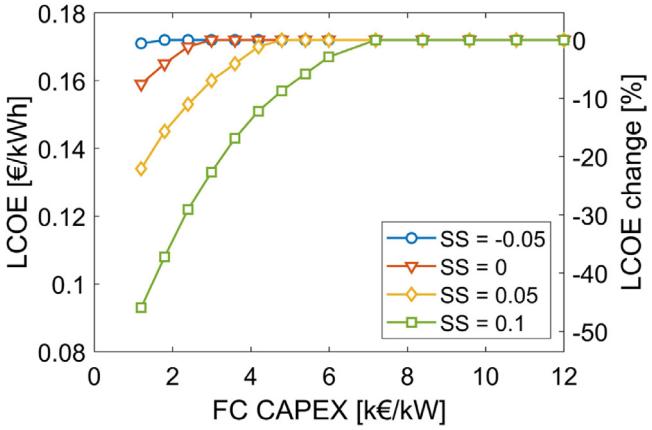

Fig. 7. LCOE as a function of the FC CAPEX for different spark spread values. The graphs refer to the current FC efficiency curve and FC stack lifetime of 5 years. The secondary *y*-axis shows the percentage change in LCOE with respect to the case with current FC CAPEX.

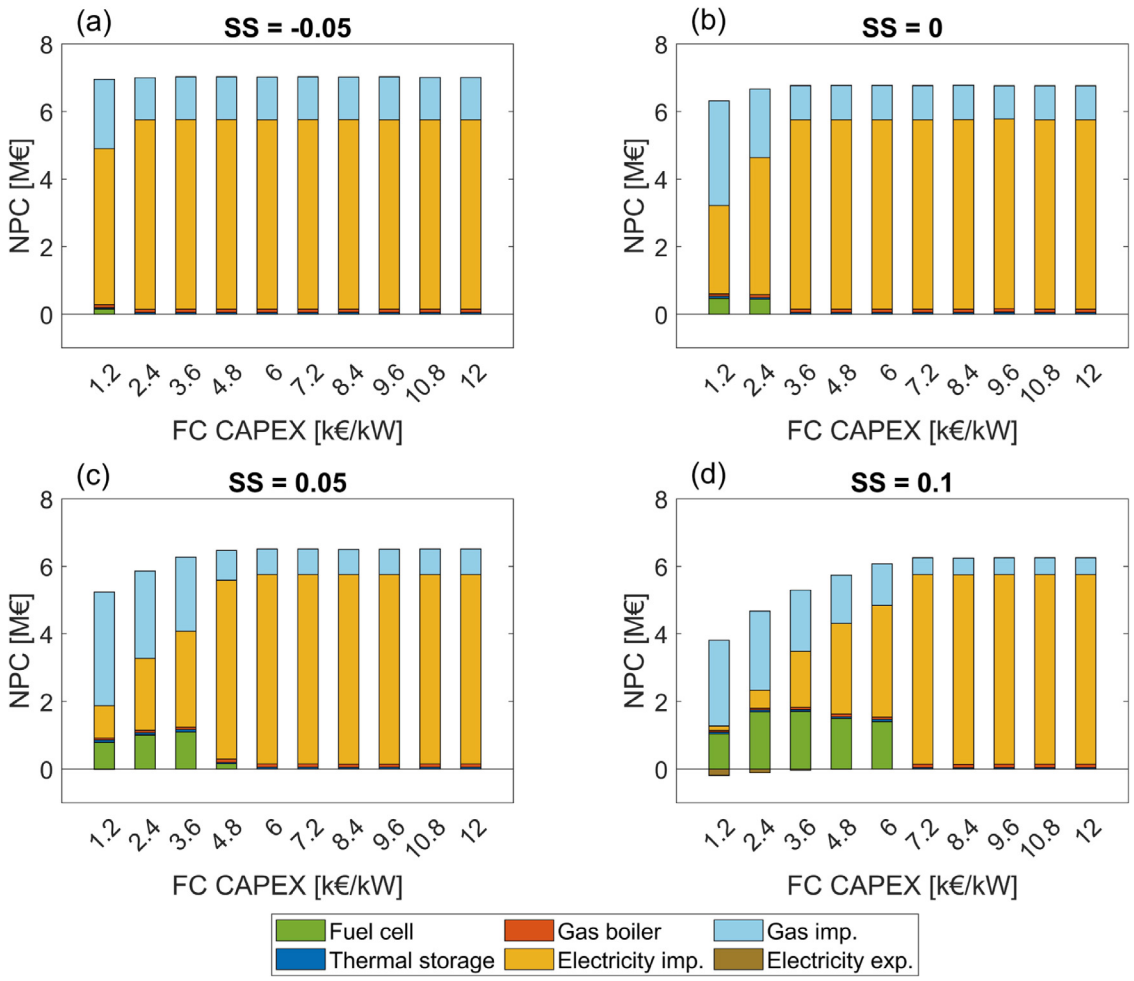

Fig. 8. Breakdown of the NPC (at the end of the project lifetime) as a function of the FC CAPEX for different spark spread values: SS = −0.05 (a), SS = 0 (b), SS = 0.05 (c), and SS = 0.1 €/kWh (d). Graphs refer to the current FC efficiency curve and FC stack lifetime of 5 years.

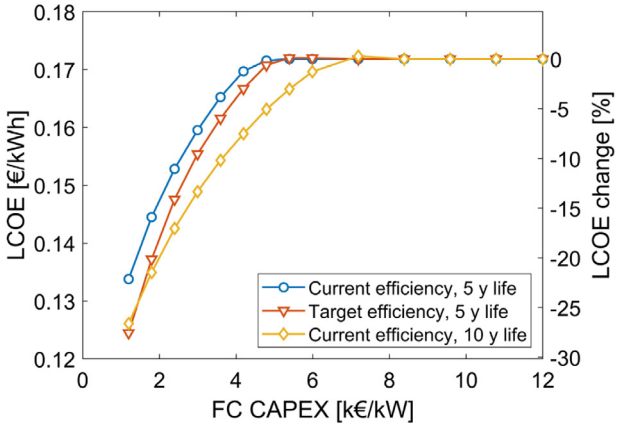

Fig. 9. LCOE as a function of the FC CAPEX by varying the FC stack lifetime and efficiency. The spark spread is set to 0.05 €/kWh. The secondary *y*-axis shows the percentage change in LCOE with respect to the case with current FC CAPEX.

6. Conclusions

This work investigates the techno-economic feasibility of SOFC-based CHP systems for non-residential buildings, with a focus on the supermarket sector. The analysis makes use of valuable data and experience from the European Comsos and DEMOSOFC projects. Real SOFC efficiency curves were implemented within the optimization framework for an accurate assessment of the SOFC performance. The main aim is to identify the conditions that allow SOFC technology to become economically viable. The following parameters have been analysed to assess their impact on the sizing results: spark spread and SOFC-related data such as investment cost, stack lifetime and efficiency.

The spark spread and the fuel cell CAPEX were shown to be key drivers for a successful business case. The higher the spark spread, the better the economic performance of the investment.

The use of SOFC systems leads to almost no advantage when the spark spread is around −0.05 €/kWh, which is close to that of Finland and Sweden. At this SS value, the FC-based CHP becomes profitable only with SOFC costs of around 1.2 to 2.4 k€/kW, which means a reduction of at least 80% of the current SOFC CAPEX. A cost of 6 k€/kW is instead sufficient for the SOFC to become profitable if SS is set to 0.1 €/kWh (around the value of Denmark, United Kingdom and Germany) and the stack lifetime is 5 years. With SS of 0.1 €/kWh and increasing the stack lifetime to the target value of 10 years, the SOFC cost-effectiveness already occurs with a CAPEX of around 9.6 k€/kW. The LCOE decreases by only 0.4% if SS is equal to −0.05 €/kWh and the FC cost is reduced from the current value (12 k€/kW) to 1.2 k€/kW (which is reasonable for scenarios with high FC production volumes). Instead, the LCOE reduction would be up to 46% with SS of 0.1 €/kWh. In scenarios with low FC CAPEX and high SS, i.e., cheap NG and expensive electricity, it was also observed that it is convenient to use the SOFC to convert NG into electricity for sale to the grid. Grid sales revenues become non-negligible with SS of 0.1 €/kWh and FC cost of around 1.2 k€/kW.

To sum up, a high spark spread is required to make the SOFC system profitable. In high SS scenarios (0.05–0.1 €/kWh), the SOFC technology can offer significant savings if a reduction in the SOFC cost occurs, which is expected in the next few years with an increase in the level of maturity of this technology.

Future steps will involve the analysis of the environmental benefits of SOFC-based cogeneration systems. Based on the optimization framework here discussed, a multi-objective optimization model will be developed to deal with both economic and environmental indicators, also considering the effect of an increase in the share of unconventional gas in the grid (e.g., biogas, biomethane and hydrogen).

Acronyms

BOP	Balance Of Plant
BS	Battery Storage
CAPEX	Capital Expenditures
CHP	Combined Heat and Power
EU	European Union
FC	Fuel Cell
GB	Gas Boiler
GHG	Greenhouse Gas
GR	Grid
LCOE	Levelized Cost Of Electricity
MILP	Mixed Integer Linear Programming
NG	Natural Gas
NPC	Net Present Cost
OPEX	Operating Expenditures
PWA	Piecewise Affine
SOC	State Of Charge
SOFC	Solid Oxide Fuel Cell
SS	Spark Spread
TMY	Typical Meteorological Year
TS	Thermal Storage

CRediT authorship contribution statement

Paolo Marocco: Conceptualization, Methodology, Software, Validation, Formal analysis, Investigation, Resources, Data curation, Writing – original draft, Visualization, Writing – review & editing. **Marta Gandiglio:** Conceptualization, Validation, Investigation, Resources, Data curation, Writing – original draft, Writing – review & editing. **Massimo Santarelli:** Writing – review & editing, Project administration, Funding acquisition.

Declaration of competing interest

The authors declare that they have no known competing financial interests or personal relationships that could have appeared to influence the work reported in this paper.

Acknowledgements

This project has received funding from the Fuel Cells and Hydrogen 2 Joint Undertaking (now Clean Hydrogen Partnership) under grant agreement No. 779481. This Joint Undertaking receives support from the European Union's Horizon 2020 research and innovation programme, Hydrogen Europe and Hydrogen Europe research.

Appendix A

The parameters $\alpha_{FC,el,i}$ and $c_{\beta,FC,el,i}$ of Eq. (12) were computed according to Eqs. (A.1) and (A.2) (Marocco et al., 2021b), for each i-th line segment of the FC performance curve (i.e., outlet electrical power as a function of the inlet gas power) with $i \in \{1, \ldots, p\}$.

$$\alpha_{FC,i} = \frac{\eta_{FC,el,i+1} \cdot z_{FC,i+1} - \eta_{FC,el,i} \cdot z_{FC,i}}{z_{FC,i+1} - z_{FC,i}} \tag{A.1}$$

$$c_{\beta_{FC,el,i}} = \left[z_{FC,i} \cdot \eta_{FC,el,i} + \frac{\left(z_{FC,i+1} \cdot \eta_{FC,el,i+1} - z_{FC,i} \cdot \eta_{FC,el,i}\right) \cdot z_{FC,i}}{z_{FC,i} - z_{FC,i+1}} \right] \cdot \frac{1}{\eta_{FC,el,p+1}} \tag{A.2}$$

where $\eta_{FC,el,k}$ and $z_{FC,k}$ represent the electrical efficiency and the fraction of the rated inlet power (in terms of gas) referred to the k-th breakpoint of the performance curve, respectively. The term p stands for the number of line segments of the curve ($p + 1$ is the total number of breakpoints).

Table A.1 reports the parameters of the PWA approximation of the SOFC performance curve. They were derived based on the electrical efficiency reported in Fig. 4. The four line-segments (i.e., 5 breakpoints) are able to accurately describe the SOFC performance curve since the relative error is always lower than 2.2%.

Table A.1
Parameters for the PWA approximation of the SOFC performance curve (outlet electrical power as a function of the inlet gas power).

z_1	z_2	z_3	z_4	z_5
0.396	0.478	0.592	0.757	1.000
η_1	η_2	η_3	η_4	η_5
0.372	0.511	0.565	0.552	0.491

Appendix B

See Fig. B.1.

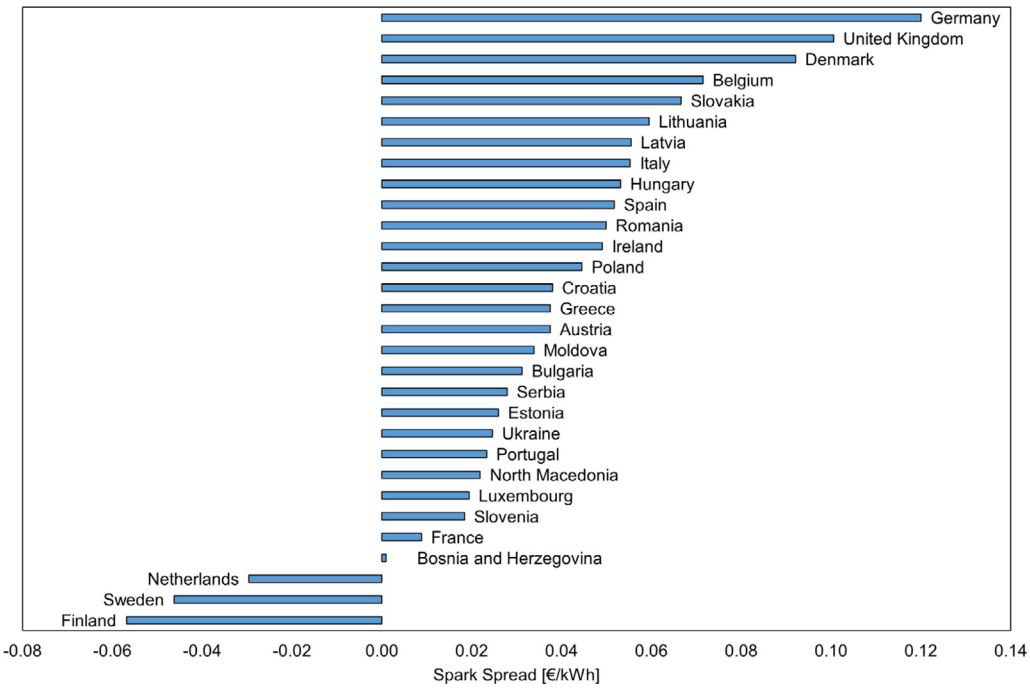

Fig. B.1. Spark Spread for European countries (evaluated from Eurostat database for non-household consumers over the last three years).

References

Accurso, F., Gandiglio, M., Santarelli, M., Buunk, J., Hakala, T., Kiviaho, J., Modena, S., Münch, M., Varkaraki, E., 2021. Installation of fuel cell-based cogeneration systems in the commercial and retail sector: Assessment in the framework of the COMSOS project. Energy Convers. Manage. 239, 114202. http://dx.doi.org/10.1016/J.ENCONMAN.2021.114202.

Adam, A., Fraga, E.S., Brett, D.J.L., 2015. Options for residential building services design using fuel cell based micro-CHP and the potential for heat integration. Appl. Energy 138, 685–694. http://dx.doi.org/10.1016/j.apenergy.2014.11.005.

Alns, A., Sleiti, A.K., 2021. Combined heat and power system based on solid oxide fuel cells for low energy commercial buildings in Qatar. Sustain. Energy Technol. Assess. 48, 101615. http://dx.doi.org/10.1016/j.seta.2021.101615.

Ammermann, H., Hoff, P., Atanasiu, M., Aylor, J., Kaufmann, M., Tisler, O., 2015. Advancing Europe's energy systems: Stationary fuel cells in distributed generation. a study for the fuel cells and hydrogen joint undertaking. https://www.fch.europa.eu/publications/advancing-europes-energy-systems-stationary-fuel-cells-distributed-generation.

Arsalis, A., 2019. A comprehensive review of fuel cell-based micro-combined-heat-and-power systems. Renew. Sustain. Energy Rev. 105, 391–414. http://dx.doi.org/10.1016/j.rser.2019.02.013.

Battelle Memorial Institute, 2016. Manufacturing cost analysis of 100 and 250 kw fuel cell systems for primary power and combined heat and power applications.

Beckers, K., Lukawski, M., Reber, T., Anderson, B., Moore, M., Tester, J., 2013. Introducing Geophires V1.0: Software package for estimating levelized cost of electri and/or heat from enhanced geothermal systems. In: Thirty-Eighth Work. Geotherm. Reserv. Eng. pp. 8.

Caramanico, N., Di Florio, G., Baratto, M.C., Cigolotti, V., Basosi, R., Busi, E., 2021. Economic analysis of hydrogen household energy systems including incentives on energy communities and externalities: A case study in Italy. Energies 14, http://dx.doi.org/10.3390/en14185847.

ComSos, 2018. Commercial scale SOFC systems. https://www.comsos.eu/. (Accessed 5 May 2022).

Crespi, E., Colbertaldo, P., Guandalini, G., Campanari, S., 2021. Design of hybrid power-to-power systems for continuous clean PV-based energy supply. Int. J. Hydrog. Energy 46, 13691–13708. http://dx.doi.org/10.1016/j.ijhydene.2020.09.152.

Ellamla, H.R., Staffell, I., Bujlo, P., Pollet, B.G., Pasupathi, S., 2015. Current status of fuel cell based combined heat and power systems for residential sector. J. Power Sources 293, 312–328. http://dx.doi.org/10.1016/j.jpowsour.2015.05.050.

European Union, 2021a. Energy performance of buildings directive. https://eur-lex.europa.eu/legal-content/EN/TXT/?uri=CELEX%3A02010L0031-20210101. (Accessed 19 May 2022).

European Union, 2021b. Energy efficiency directive. https://eur-lex.europa.eu/legal-content/EN/TXT/?uri=CELEX%3A02012L0027-20210101. (Accessed 19 May 2022).

Eurostat - Data Explorer, 2022a. Electricity prices for non-household consumers - bi-annual data (from 2007 onwards). http://appsso.eurostat.ec.europa.eu/nui/show.do?dataset=nrg_pc_205&lang=en. (Accessed 17 March 2022).

Eurostat - Data Explorer, 2022b. Gas prices for non-household consumers - bi-annual data (from 2007 onwards). http://appsso.eurostat.ec.europa.eu/nui/show.do?dataset=nrg_pc_203&lang=en. (Accessed 17 March 2022).

Ferroli Industrial Heating, 2021. 2021 Technical catalogue.

Fong, K.F., Lee, C.K., 2016. System analysis and appraisal of SOFC-primed micro cogeneration for residential application in subtropical region. Energy Build. 128, 819–826. http://dx.doi.org/10.1016/j.enbuild.2016.07.060.

Fubara, T.C., Cecelja, F., Yang, A., 2014. Modelling and selection of micro-CHP systems for domestic energy supply: The dimension of network-wide primary energy consumption. Appl. Energy 114, 327–334. http://dx.doi.org/10.1016/j.apenergy.2013.09.069.

Gabrielli, P., 2019. Optimal Design of Multi-Energy Systems: From Technology Modeling to System Optimization. ETH Zurich.

Gabrielli, P., Flamm, B., Eichler, A., Gazzani, M., Lygeros, J., Mazzotti, M., 2016. Modeling for optimal operation of PEM fuel cells and electrolyzers. In: EEEIC 2016 - Int. Conf. Environ. Electr. Eng. IEEE, pp. 1–7. http://dx.doi.org/10.1109/EEEIC.2016.7555707.

Gabrielli, P., Gazzani, M., Martelli, E., Mazzotti, M., 2018. Optimal design of multi-energy systems with seasonal storage. Appl. Energy 219, 408–424. http://dx.doi.org/10.1016/j.apenergy.2017.07.142.

Gandiglio, M., Lanzini, A., Santarelli, M., Acri, M., Hakala, T., Rautanen, M., 2020. Results from an industrial size biogas-fed SOFC plant (the DEMOSOFC project). Int. J. Hydrog. Energy 45, 5449–5464. http://dx.doi.org/10.1016/j.ijhydene.2019.08.022.

Gandiglio, M., Lanzini, A., Santarelli, M., Leone, P., 2014. Design and optimization of a proton exchange membrane fuel cell CHP system for residential use. Energy Build. 69, 381–393. http://dx.doi.org/10.1016/j.enbuild.2013.11.022.

Gandiglio, M., Santarelli, M., Münch, M., Modena, S., Varkaraki, E., Hakala, T., Fontell, E., 2018. Deliverable 5.2: Techno-economic models of the considered SOFC-based CHP systems - ComSos "commercial-scale SOFC systems".

Gestore Mercati Energetici (GME), 2022. Statistiche - dati di sintesi MPE-MGP. https://www.mercatoelettrico.org/It/Statistiche/ME/DatiSintesi.aspx. (Accessed 17 March 2022).

Giarola, S., Forte, O., Lanzini, A., Gandiglio, M., Santarelli, M., Hawkes, A., 2018. Techno-economic assessment of biogas-fed solid oxide fuel cell combined heat and power system at industrial scale. Appl. Energy 211, 689–704. http://dx.doi.org/10.1016/j.apenergy.2017.11.029.

Gracia, L., Casero, P., Bourasseau, C., Chabert, A., 2018. Use of hydrogen in off-grid locations, A techno-economic assessment. Energies 11, 3141. http://dx.doi.org/10.3390/en11113141.

Hormaza-Mejia, A., Zhao, L., Brouwer, J., 2017. SOFC micro-CHP system with thermal energy storage in residential applications. In: Proc. ASME 2017 15th Int. Conf. Fuel Cell Sci. Eng. Technol. FUELCELL 2017. pp. 1–6. http://dx.doi.org/10.1115/FUELCELL2017-3142.

IEA, 2019. Perspectives for the clean energy transition. The critical role of buildings. https://www.iea.org/reports/the-critical-role-of-buildings.

Jing, R., Wang, M., Brandon, N., Zhao, Y., 2017. Multi-criteria evaluation of solid oxide fuel cell based combined cooling heating and power (SOFC-CCHP) applications for public buildings in China. Energy 141, 273–289. http://dx.doi.org/10.1016/j.energy.2017.08.111.

Lamagna, M., Nastasi, B., Groppi, D., Rozain, C., Manfren, M., Astiaso Garcia, D., 2021. Techno-economic assessment of reversible solid oxide cell integration to renewable energy systems at building and district scale. Energy Convers. Manage. 235, 113993. http://dx.doi.org/10.1016/j.enconman.2021.113993.

Langnickel, H., Rautanen, M., Gandiglio, M., Santarelli, M., Hakala, T., Acri, M., Kiviaho, J., 2020. Efficiency analysis of 50 kWe SOFC systems fueled with biogas from waste water. J. Power Sources Adv. 2, 100009. http://dx.doi.org/10.1016/j.powera.2020.100009.

Market Observatory for Energy, 2019. Quarterly report on European electricity markets.

Marocco, P., Ferrero, D., Lanzini, A., Santarelli, M., 2019. Benefits from heat pipe integration in H 2/H 2 O fed SOFC systems. Appl. Energy 241, 472–482. http://dx.doi.org/10.1016/j.apenergy.2019.03.037.

Marocco, P., Ferrero, D., Lanzini, A., Santarelli, M., 2021a. Optimal design of stand-alone solutions based on RES + hydrogen storage feeding off-grid communities. Energy Convers. Manage. 238, 114147. http://dx.doi.org/10.1016/j.enconman.2021.114147.

Marocco, P., Ferrero, D., Martelli, E., Santarelli, M., Lanzini, A., 2021b. An MILP approach for the optimal design of renewable battery-hydrogen energy systems for off-grid insular communities. Energy Convers. Manage. 245, 114564. http://dx.doi.org/10.1016/j.enconman.2021.114564.

McLarty, D., Brouwer, J., Ainscough, C., 2016. Economic analysis of fuel cell installations at commercial buildings including regional pricing and complementary technologies. Energy Build. 113, 112–122. http://dx.doi.org/10.1016/j.enbuild.2015.12.029.

McPhail, S.J., Kiviaho, J., Conti, B., 2017. The Yellow pages of SOFC technology - International status of SOFC deployment 2017. https://www.enea.it/en/publications/abstract/the-yellow-pages-of-sofc-technology.

Naimaster, E.J., Sleiti, A.K., 2013. Potential of SOFC CHP systems for energy-efficient commercial buildings. Energy Build. 61, 153–160. http://dx.doi.org/10.1016/j.enbuild.2012.09.045.

Napoli, R., Gandiglio, M., Lanzini, A., Santarelli, M., 2015. Techno-economic analysis of PEMFC and SOFC micro-CHP fuel cell systems for the residential sector. Energy Build. 103, 131–146. http://dx.doi.org/10.1016/j.enbuild.2015.06.052.

Rubel, F., Brugger, K., Haslinger, K., Auer, I., 2017. The climate of the European Alps: Shift of very high resolution Köppen-Geiger climate zones 1800-2100. Meteorol. Z. 26, 115–125. http://dx.doi.org/10.1127/metz/2016/0816.

Schopfer, S., Tiefenbeck, V., Staake, T., 2018. Economic assessment of photovoltaic battery systems based on household load profiles. Appl. Energy 223, 229–248. http://dx.doi.org/10.1016/j.apenergy.2018.03.185.

Sorace, M., Gandiglio, M., Santarelli, M., 2017. Modeling and techno-economic analysis of the integration of a FC-based micro-CHP system for residential application with a heat pump. Energy 120, 262–275. http://dx.doi.org/10.1016/j.energy.2016.11.082.

Steen, D., Stadler, M., Cardoso, G., Groissböck, M., DeForest, N., Marnay, C., 2015. Modeling of thermal storage systems in MILP distributed energy resource models. Appl. Energy 137, 782–792. http://dx.doi.org/10.1016/j.apenergy.2014.07.036.

Tan, L., Dong, X., Gong, Z., Wang, M., 2018. Analysis on energy efficiency and CO2 emission reduction of an SOFC-based energy system served public buildings with large interior zones. Energy 165, 1106–1118. http://dx.doi.org/10.1016/j.energy.2018.10.054.

Whiston, M.M., Lima Azevedo, I.M., Litster, S., Samaras, C., Whitefoot, K.S., Whitacre, J.F., 2021. Paths to market for stationary solid oxide fuel cells: Expert elicitation and a cost of electricity model. Appl. Energy 304, http://dx.doi.org/10.1016/j.apenergy.2021.117641.

Wilson, E., 2014. OEDI: Commercial and Residential Hourly Load Profiles for All TMY3 Locations in the United States. Natl. Renew. Energy Lab., http://dx.doi.org/10.25984/1788456.